Journal of Sound and Vibration 329 (2010) 3030–3040

Contents lists available at ScienceDirect

Journal of Sound and Vibration

journal homepage: www.elsevier.com/locate/jsvi

Influence of ballast models in the dynamic response of railway viaducts

Constança Rigueiro [a], Carlos Rebelo [b,*], Luís Simões da Silva [b]

[a] Department of Civil Engineering, EST—Institute Polytechnic of Castelo Branco, Av. Do Empresário, 6000-767 Castelo Branco, Portugal
[b] Department of Civil Engineering, FCT—University of Coimbra, University Campus 2, 3030-788 Coimbra, Portugal

ARTICLE INFO

Article history:
Received 14 July 2008
Received in revised form
25 January 2010
Accepted 1 February 2010
Handling Editor: A.V. Metrikine
Available online 1 March 2010

ABSTRACT

This paper presents an investigation of the numerical, dynamic response of medium-span railway viaducts by taking into account the influence of the ballasted track and the loadmodelling methodologies. Three models for the track and two loading procedures (the Moving Forces procedure and the Train–Structure Interaction procedure) were used. The comparison was made using three case studies. Model calibration using available response-acceleration measurements showed that time variation of the first natural frequency must be assumed to reproduce the measured time histories. The influence of track models was detectable in the time domain for only the maximum accelerations. When response is analysed in the frequency domain, results show that track models act as a filter for the high-frequency components. When the Moving Forces load model was used, the effect of the track models was less significant but consistent with the previous conclusion.

1. Introduction

The dynamic response of railway bridges subjected to moving vehicles has been an increasingly popular topic of research in recent years, and many scientists and engineers have studied the effect of high-speed traffic [10,19,20,22]. The European Rail Research Institute (ERRI) has also conducted research and proposed rules for the design of railway bridges [5]. In its final report [8], Committee D214 of the ERRI pointed out the importance of field measurements in the calibration and validation of the finite element (FE) models of the railway bridges and the techniques used to predict their dynamic response.

According to EN 1990 [6], whenever a dynamic analysis is required for a railway bridge, it is necessary to verify the maximum peak deck acceleration due to rail traffic as a safety criteria for the prevention of track instability. The frequency band considered in the dynamic calculations should range from 0 to 30 Hz, or 1.5 times the frequency of the first mode shape of the structural element being analysed. For this reason, the mode superposition method is often used in the dynamic calculations of the railway bridge response because it allows the limitation of the frequency range.

The methodologies used to compute the response accelerations of railway bridges due to the passage of trains are usually based on one of two loading strategies: the Moving Forces and the Train–Structure Interaction load models. In the first and simpler model, the solution of a system of linear differential equations gives the dynamic structural system response; while in the second model, a system of nonlinear equations must be solved in order to calculate the contact

* Corresponding author.
E-mail addresses: constanca@est.ipcb.pt (C. Rigueiro), crebelo@dec.uc.pt (C. Rebelo), luisss@dec.uc.pt (L. Simões da Silva).

0022-460X/$ - see front matter © 2010 Elsevier Ltd. All rights reserved.
doi:10.1016/j.jsv.2010.02.002

forces between the train and the rails. If the railway platform (composed of the ballast, the rails, and the sleepers) is also included in the model, the numerical formulation becomes more complex but has the advantage of allowing the evaluation of the platform's influence on the bridge response acceleration.

Field measurements and the subsequent modal identification (previously carried out by the authors on several simply supported viaducts with medium spans [16,17,18]) showed that the presence of the railway platform, particularly the ballast, on the viaducts influences the boundary conditions of the deck in two places: (i) at the simply supported ends of the decks, where some continuity over the end support introduces a moment of resistance; and (ii) along the longitudinal contact sides of the twin, structurally independent decks used for each traffic direction, where a flexible connection between both twin decks is introduced.

To evaluate the influence of the railway platform on the dynamic response of the viaduct models and to obtain numerical acceleration responses to the passage of trains which can be compared with field measurements, a numerical investigation was performed. It focused on the influence of ballast on the computation of the dynamic-response acceleration of medium-span viaducts. Since the numerical system may include train–structure interaction, the step-by-step, direct-time integration method must be carefully chosen.

2. Modelling the railway ballasted track

2.1. General overview

The FE models of the railway-ballasted track include elements for the ballast, rails, sleepers, and the connections between the rails and sleepers. Each element fulfils specific functions and contributes toward the functional behaviour of the whole track when subjected to the passage of the trains.

The rails are an important component in the track structure that transfer the wheel loads; distribute them over the sleepers and supports; guide the wheels in the lateral direction; provide a smooth running surface; and distribute acceleration and braking forces over the supports.

The sleepers, usually made of timber or concrete, are elements positioned just below the rails. They provide support for the rails by sustaining rail forces and transferring them as uniformly as possible to the ballast. The connections between the rail and the sleeper enable the transfer of both vertical and horizontal rail forces (with respect to the sleepers), dampen the vibrations and impacts caused by the moving traffic, and retain the track gauge and rail inclination within certain tolerances.

Finally, the ballast bed consists of a layer of a coarse-sized, non-cohesive, and granular material. Traditionally, angular, crushed, hard stones, and rocks have been considered as the good ballast materials. The interlocking of ballast grains and their confined conditions inside the ballast bed permit the load distribution and damping. They also provide the lateral and longitudinal support of the track as well as drainage. The thickness of the ballast bed should allow the sub-grade to be loaded as uniformly as possible. The usual depth for the ballast is about 0.3 m measured from the underside of the sleeper [9].

In earlier studies, models of the ballasted track were developed in order to investigate the deflections of the track due to the passage of a train. More recently, the train/track interaction problem was also investigated—this time considering the wheel/rail contact forces and the irregularities of the track. A review of these studies is presented in the literatures [12,15,21].

A large variety of ballasted track models can be found in the literature, from the simple 2D to the more complex 3D models [7,20,21]. The common characteristic between them is the presence of vertical springs and dampers, connected in parallel, to simulate the stiffness and damping of the platform's elements. The rails are modelled as infinite Bernoulli–Euler or Timoshenko beams, and in the 3D models, both rails are taken into account and bending and shear deformation of the sleepers are included. Some of these models consider the masses of the sleepers and ballast as point masses located below each sleeper, and shear springs and dampers may interconnect these masses [21]. The values of the mechanical properties of the track components, such as mass, inertia, and elasticity, are an essential input for dynamic track behaviour and, of course, for the study of the interaction between the train and track.

To compare the numerical results with the dynamic response obtained from the field measurements, 2D and 3D models were considered, for one of the analysed viaducts, the torsional effects cannot be neglected.

2.2. Models and parameters

The general model of ballasted tracks is presented in Fig. 1. Track Model III [8] includes all the components shown in the figure. For the sake of comparison, two additional, simpler models (I and II) were investigated. Although parameter values obtained from the literature present high variability, the values presented in Table 1 were chosen to be the representative of the three models. They were used in this investigation and implemented in the finite element models of the viaducts. The parameters were considered to remain constant along the railway track.

In Model I [20], only the elements for the rail and the connection between the rail and structure are present. In this model, rails were considered as infinitely long beams with both axial stiffness and in-plane and out-of-plane flexural

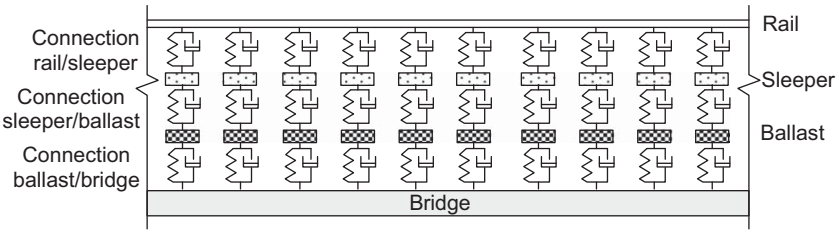

Fig. 1. Ballasted track model.

Table 1
Properties of the models I, II, and III [8,14,20].

	Model I	Model II	Model III
Rail UIC60			
Young's modulus E_r ($N\,m^{-2}$)		210E+09	
Density ρ_r ($kg\,m^{-3}$)		7850	
Flexural inertia I_r (m^4)		3055E+08	
Section area A_r (m^2)		76.9E−04	
Connection rail/sleeper			
Vertical stiffness K_{rp} ($N\,m^{-1}$)	–	300E+06	500E+06
Vertical damping C_{rp} ($N\,s\,m^{-1}$)	–	80E+03	200E+03
Sleeper			
Mass M_s (kg)	–	300	290
Length between sleepers d_s (m)	–	0.6	0.6
Ballast			
Vertical stiffness K_{bv} ($N\,m^{-1}$)	104E+06	120E+06	–
Vertical damping C_{bv} ($N\,s\,m^{-1}$)	50E+03	114E+03	–
Horizontal stiffness K_{bh} ($N\,m^{-1}$)	104E+05	–	–
Horizontal damping C_{bh} ($N\,s\,m^{-1}$)	50E+03	–	–
Vertical stiffness ballast/sleeper K_{bs} ($N\,m^{-1}$)	–	–	538E+06
Vertical damping ballast/sleeper C_{bs} ($N\,s\,m^{-1}$)	–	–	120E+03
Mass M_b (kg)	–	–	412
Vertical stiffness ballast/bridge K_{bb} ($N\,m^{1}$)	–	–	1000E+06
Vertical damping ballast/bridge C_{bb} ($N\,s\,m^{-1}$)	–	–	50E+03

stiffness. Linear springs and dampers in the vertical and longitudinal directions, located 1 m apart from each other, represent the joint effect of the sleepers and ballast.

In addition to the parameters set forth in Models I and II [14] considered the sleeper as a suspended mass and the connections between the rails and the sleepers as linear springs and viscous dampers acting in parallel. Their elastic and viscous properties were determined by the material properties and the manufacturing processes. The equivalent stiffness of both springs acting in series was about 86 MN/m compared to the stiffness of 104 MN/m given for Model I.

In Model III [8], the mass of the ballast was included as a point mass instead of as a distributed mass, and additional springs and dampers were used to simulate the connection between the bridge and ballast. As a result, this model, which has three springs in series, had an equivalent stiffness of about 206 MN/m, considerably stiffer than Models I and II.

It is worth noticing that, in Table 1, the equivalent stiffness of springs related to ballast is between 104 MN/m (Model I) and 350 MN/m (Model III). Previously, Zhai et al. [21] presented a calibrated model with a ballast stiffness value located in the range of results (110–185 MN/m) obtained in a full-scale ballasted track model at the Railway Institute of Tongji University in Shanghai, China. The same authors [21] compared the influence of ballast shear parameters obtained in Swedish Railways (K_b=717 MN/m and C_b=173 kNs/m) and the ballast shear parameters used in Chinese Railways (K_b=78.4 MN/m and C_b=80 kNs/m), concluding that the ballast accelerations were about 23% larger in the softer model.

3. Modelling the railway viaducts

3.1. General description

The characteristics of the three viaducts used to perform the analysis and the results obtained from the measurements performed during train passages were comprehensively described in our previous study [17]. The viaducts had spans

varying from 11.44 to 23.50 m and were all composed of single-span, simply supported, twin slabs, laying side-by-side (one for each traffic direction). The geometric characteristics of each slab are summarized in Table 2 and in Fig. 2, which represents the generic-plan view of the viaducts and the structural layout of a pre-stressed concrete slab with slightly variable depth and an average mass per unit length of about 21 ton m^{-1}.

The ballast had an average depth of 0.60 m, depending on the slab thickness, and was located throughout the width of the twin slabs. The bearing supports, two at each extremity of the deck, were made of steel pots filled with rubber material and were considered free to rotate. There was no continuity of the slab over the supports of the abutments, except for the one created by the ballast track. It must be emphasized that for Viaducts 1 and 8, the line of supports was not collinear when considering both decks, and Viaduct 12 was skewed relative to the longitudinal axis.

3.2. Modal identification based FE models of the viaducts

The finite element models of the viaducts were developed and calibrated using the modal information, namely the first three natural frequencies and mode shapes, obtained from measurements [16,17].

Although the structural model used in the original design of the viaducts corresponded to simply supported decks, the experimental modal analysis showed that the viaducts behave as simply supported slabs with some flexural stiffness at the supports. This stiffness was provided by the track's continuity over the supports, and thus the finite element model included two horizontal springs over the supports.

The concrete properties used in the computations were the specific weight, γ_c=25 kN m^{-3}, and the Young's modulus, E_b=54.6 GPa. For the ballast, the specific weight, γ_b=20 kN m^{-3}, was considered.

For the first two Viaducts, 1 and 8, a 2D-model of the structure and the vehicles were adequate to fit the dynamic behaviour, since the significant natural mode shapes did not include torsional deformations. The mode shapes corresponded to the first three modes of a beam with flexural stiffness over the supports, and the values of the respective natural frequencies are given in Table 3. These values are in good agreement with those from the modal identification performed previously [17].

Since Viaduct 12 was composed of two side-by-side skew slabs, coupled modes of both slabs were identified. They showed a duplication of the frequency peaks corresponding to symmetrical and non-symmetrical shapes with reference to the contact plan between the slabs (Fig. 3). Furthermore, torsion of the decks was present in all mode shapes. The separation between the corresponding natural frequencies depended directly on the shear stiffness of the connection between the slabs, which was composed of the ballast only. This coupling effect allowed the quantification of the ballast shear stiffness from the measurements in Ref. [17] with the value G_b=35 MPa. When a Poisson's ratio of 0.2 and

Table 2
Geometric characteristics of the viaducts.

Viaduct	Span (m)	Width (m)	HL (m)	H (m)	HR (m)	α (deg.)
1	23.50	5.14	0.92	1.14	0.91	90
8	21.00	4.23	1.05	1.15	1.05	90
12	11.44	4.54	0.70	0.90	0.70	63.9

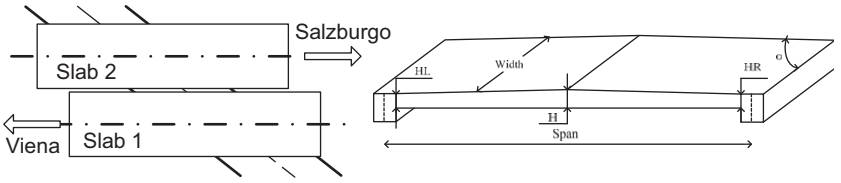

Fig. 2. Plan view of the viaducts: twin slabs and structural layout.

Table 3
Computed and measured natural frequencies for Viaducts 1 and 8.

Viaduct	Modes	Frequency (Hz)	Measured frequency (Hz)
1	1st	4.40	4.8
	2nd	13.70	13.3
	3rd	28.75	27.7
8	1st	5.44	5.4
	2nd	17.74	18.8
	3rd	37.16	37.4

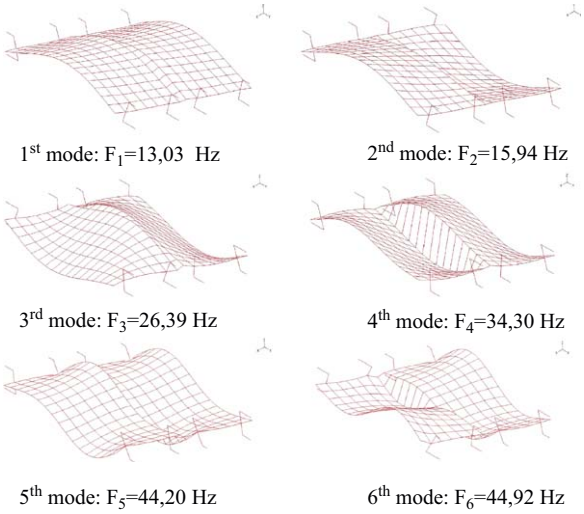

Fig. 3. Mode shapes of the 3D finite element model for Viaduct 12.

Table 4
Computed and measured natural frequencies for Viaduct 12.

Modes	Frequency (Hz)	Measured frequencies (Hz)
1st–2nd	13.03–15.94	13.7–16.5
3rd–4th	26.39–34.30	26.2–29.4
5th–6th	44.20–44.92	41.4–43.6

homogeneous elastic behaviour of the ballast were considered, the resulting equivalent vertical stiffness of equally spaced linear springs was 84 MN/m. This compared well with the equivalent vertical stiffness of Model II's vertical springs given in the previous Section.

The 3D FE model developed for this viaduct included the twin slabs connected by vertical springs and the supports with partial moment restriction. The eigenmodes of this finite element model are represented in Fig. 3, and the corresponding values of the first four pairs of natural frequencies are given in Table 4. They are in good agreement with those obtained from the measurements [16,17].

4. Numerical simulation of the loading

The two different loading models used to compute the viaducts' acceleration response when subjected to the real traffic (the Moving Forces and the Train–Structure Interaction) are represented in Fig. 4. The vehicle in Fig. 4a represents a conventional, real train. Each bogie has two axles represented by two forces in the Moving Forces model (Fig. 4b and Table 5). For the Interaction model, the vehicle was replaced by a two dof, spring–mass system consisting of the mass M_v, supported by a linear spring, and a damper, of mass $M_{w,}$ connected in parallel (Fig. 4c and Table 6). The stiffness and damping of this system, denoted by K_v and C_v, respectively, corresponded to the primary suspension of the train vehicle. The lumped mass M_v corresponded to a quarter of the mass of the car body and one-half of the bogie mass, while the mass M_w corresponded to the mass of the wheel. The characteristic length of the carriage is denoted by D_k. It was assumed that the train crosses the bridge at a constant speed.

When comfort requirements related to the vehicle behaviour had to be checked, Train–Structure Interaction models were used in the computations instead of the simpler Moving Forces models. To achieve this, contact algorithms can be used. However, the accurate computation of dynamic contact between elastic bodies becomes complex due to the rapid variation of acceleration, velocity, and stress fields in elastic bodies [2,11,13]. On the other hand, the numerical analysis of dynamic problems using the Newmark algorithm with the Trapezoidal Rule is stable for linear analysis but becomes unstable during the dynamic contact. Therefore, it was necessary to introduce numerical dissipation into the time-step analysis to control the oscillations resulting from the gap constraints at the points of contact. Moreover, the integration scheme was required to dissipate the high frequencies generated by the compatibility of the displacements in the contact surfaces [2,13].

ADINA software [1,3,4], especially the contact algorithm, was used to model the interaction between the train and the structure. The step-by-step response acceleration of the viaducts was computed using the Wilson-θ method.

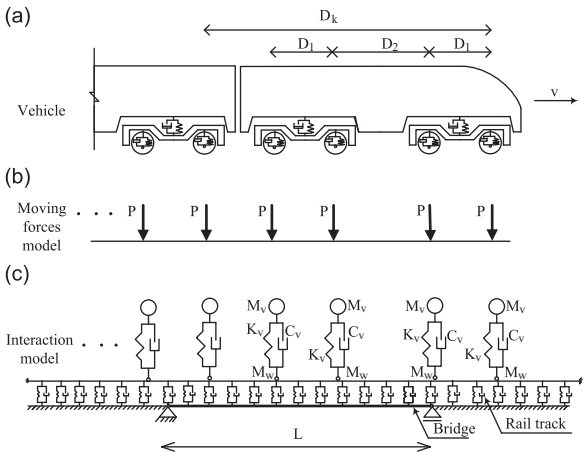

Fig. 4. (a) Vehicle dynamic model; (b) Moving Forces; and (c) Interaction load models.

Table 5
Characteristics of Moving Forces load model for different trains and locomotives.

Viaduct	Real trains investigated	D_1 (m)	D_2 (m)	D_k (m)	F_{locom} (kN)	$F_{carriages}$ (kN)	Speed (km h^{-1})
1	Locomotive 1116 (only)	3.0	6.9	–	210.93	–	130
	Train ICE (7 vehicles)	2.5	15.8	26.4	204.05	127.53	140
8	Locomotive 1047 (only)	3.0	6.9	–	215.0	–	85
	Train EC (10 vehicles)	3.0	6.9	–	210.93	–	159
		2.5	16.5	28.4 (1st carriage)	–	127.53	
		2.5	16.5	26.4 (remaining carriages)	–	135.62	
12	Locomotive 1116 (only)	3.0	6.9	–	210.93	–	150

Table 6
Parameters for the Interaction model.

Real train		K_v (N/m)	C_v (Ns/m)	M_v (ton)	M_w (ton)
ICE Train (7 vehicles)	Power car	4800E3	108E3	18.8	2.0
	Carriages	1600E3	20E3	11.05	1.95

The numerical simulations were carried out using the characteristics of real trains for which measurements of the response accelerations were available. In general, the response to the passage of a single locomotive and of a complete high-speed train was chosen. The characteristics and crossing speeds of the vehicles, measured with a speedometer as the trains passed over the viaducts, are summarized in Table 5.

5. Dynamic response due to train passage

Figs. 5–12 The accelerations computed with the numerical models were compared with the previously reported field measurements [17]. The Moving Forces Model was used in all case studies and the Interaction Model was used only for Viaduct 1, since the vehicle parameters were not available for the trains considered in the analysis of Viaducts 8 and 12. Figs. 5, 7, 9, and 11 compare the measured response to the response acceleration in the time domain in the mid-span region of the viaducts. Figs. 6, 8, 10, and 12 show the frequency domain representation of the computed response with different track models. Coefficients of viscous damping obtained from the measurements [17] were used in the calculations.

When analysing the time-response acceleration of all the study cases, two different time slots were clearly identified. The first corresponded to the forced response during the train's passage over the viaduct, and the second corresponded to the free vibration after the train left the viaduct. During the free vibration, the comparison between computed and measured responses was obviously not influenced by the loading model used and the differences between track model types. Rather, the pertinent influence seemed to be the presence of the rails, which was common to all track models considered and resulted in an increase in bending stiffness. The differences between measured and computed response were mainly due to period elongation of the computed oscillation decay relative to the measured response. This effect was

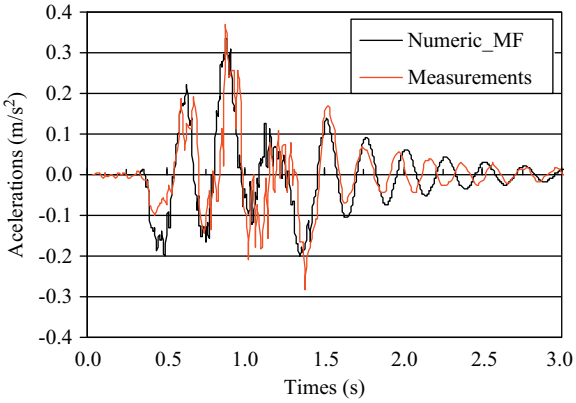

Fig. 5. Numeric and measured response acceleration for Viaduct 1 and locomotive 1116 and Moving Forces load model and Track Model III.

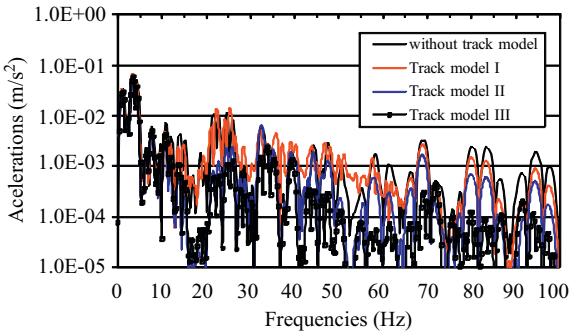

Fig. 6. Frequency domain representation of numerical response acceleration at mid-span of viaduct 1 due to locomotive 1116 and Moving Forces load model.

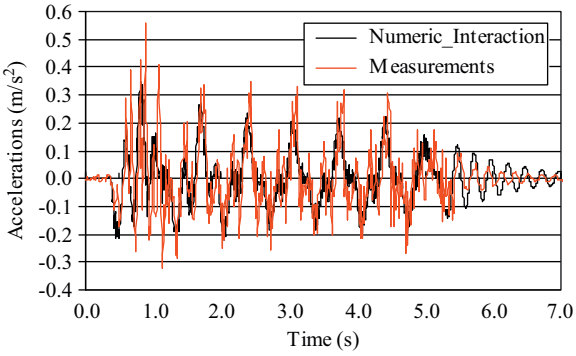

Fig. 7. Numeric and measured response acceleration for Viaduct 1 and ICE549 train and Interaction load model and Track Model III.

observed in all the calculated responses and corresponded to a lower first natural frequency of the structural model in comparison to reality.

Two main factors contributed to these differences. The first is related to the way the mass of the vehicles is taken into account. Since this mass was included in models by adding mass to the viaducts, it remained in the model after the train left the viaduct thereby decreasing the numerical first natural frequency by about 7%. The second factor must be the nonlinear behaviour of the deck, since stiffness decreased when subjected to intense vibration during the train passage and increased thereafter when the vibration amplitudes diminished. This behaviour must be due to the presence of the ballasted track, since the deformations in the pre-stressed concrete deck were sufficiently low to remain in the elastic range. Depending on the interlocking forces within the ballast, relative movements of the particles may have occurred during the train passage and consequently, the stiffness decreased. This conclusion is also supported by the fact that, when very low amplitudes of ambient vibration were used in the modal identification, the first natural frequency could

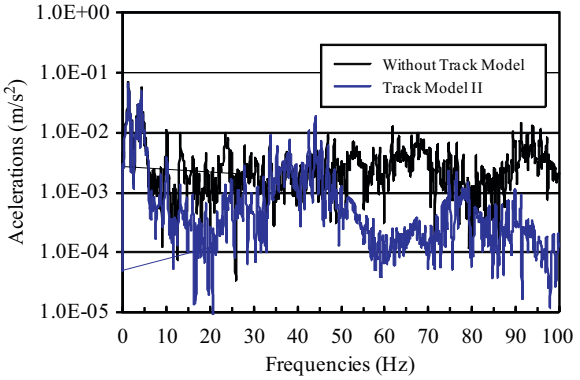

Fig. 8. Frequency domain of numerical response acceleration at mid-span of Viaduct 1 due to ICE549 train and Interaction load model and Track Model II.

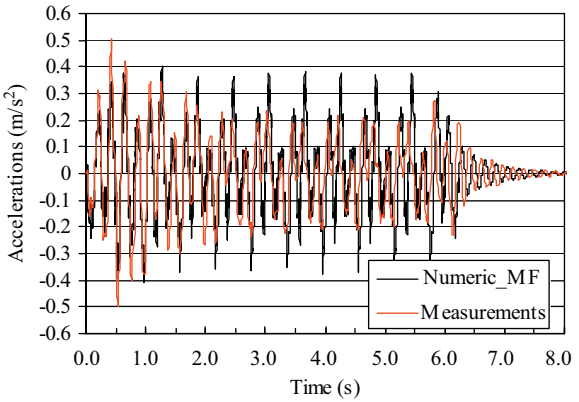

Fig. 9. Numeric and measured response acceleration for Viaduct 8 and EC train and Moving Forces load model and Track Model III.

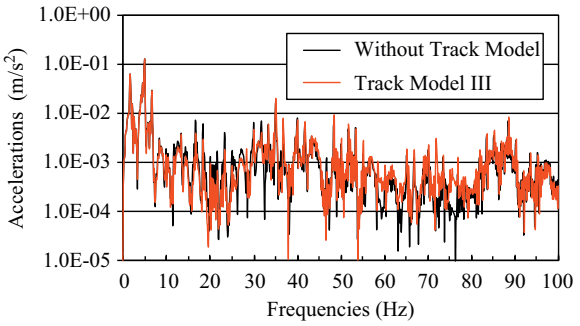

Fig. 10. Frequency domain representation of numerical response acceleration at mid-span of Viaduct 8 due to EC train and; Moving Forces load model and Track Model III.

increase up to 30% compared to one obtained with larger free vibration amplitudes measured immediately after the train's passage [17].

As a conclusion, when measured and computed forced vibrations were compared during the train's passage, the natural frequencies decreased due to the added mass from the train and decrease in ballast stiffness. This must be considered in the computations performed to obtain the numerical response.

Another important conclusion of this analysis is that special care should be taken whenever low-amplitude, free-vibration measurements, e.g. from ambient vibration, are used to identify eigenfrequencies of railway viaducts for the purpose of checking maximum accelerations of the deck. Given the analyses conducted, it is probable that at least the first natural frequency will be overestimated.

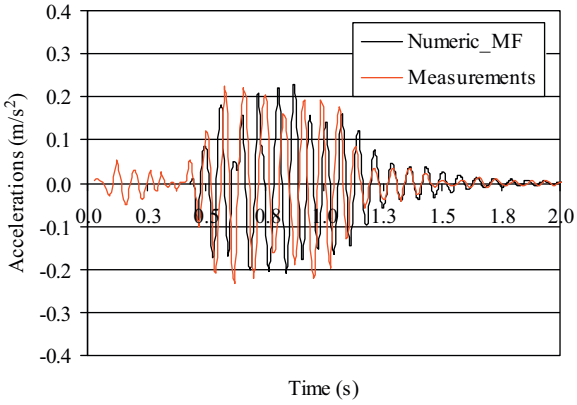

Fig. 11. Numeric and measured response acceleration for Viaduct 12 and locomotive 1116 and Moving Forces load model and Track Model III.

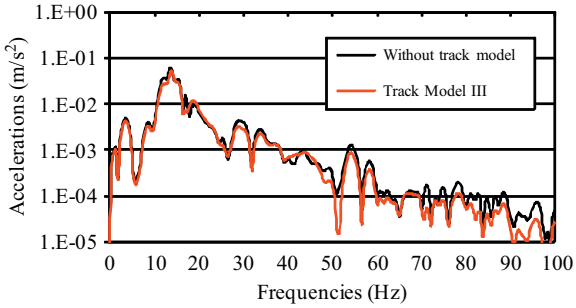

Fig. 12. Frequency domain representation of numerical response acceleration at mid-span of Viaduct 12 due to locomotive 1116 and Moving Forces load model and Track Model III.

6. Numerical evaluation of the influence of the track model

The forced response acceleration of the viaducts was analysed when a single locomotive or a complete train passed over the structures. After analysing the evolution of the time histories (Figs. 7, 9 and 11) during the forced vibration, it was concluded that the numerical response fit the measurements quite well, except for the high frequencies. Although not represented in the figures, the results obtained for the different track models looked similar when observed in the time domain. Considering the frequency-domain representation of the numerical results (Figs. 6, 8 and 10), a general conclusion was that the influence of the models can be relevant only in frequency components higher than approximately 15 Hz. When present, the influence of the track models tended to reduce the contribution of the frequency components thereby acting as a filter (Figs. 6 and 8).

The Fourier spectra of Viaduct 1's response acceleration due to the passage of a locomotive type 1116 and a German ICE train are shown in Figs. 6 and 8, respectively. In the locomotive loading case (Fig. 6), it can be seen that track models exert different influences on the acceleration response of the bridge in higher frequencies. The track models had similar behaviour in the lower frequency range (up to 15 Hz) but for higher frequencies, Track Model III was the most efficient in filtering out these frequency components.

Fig. 8 shows the response acceleration during the passage of the ICE train with seven vehicles at a speed of 140 km/h. After the analysis, it was concluded that, independent of the load model used, none of the three ballast track models significantly influenced the acceleration response in the lower frequency range up to about 15 to 20 Hz. In addition, Models II and III performed better concerning numerical dissipation of the higher frequencies. This behaviour was emphasized when the Interaction load model was used in the calculations instead of the Moving Forces load model.

The analysis made for Viaduct 8 followed the same methodology as for Viaduct 1. A locomotive type 1047 and an EC train with 10 vehicles were considered. Only the Moving Forces load model was used since vehicle parameters needed for the Interaction model were not available.

Ballast track models showed similar behaviour as in Viaduct 1, although the effect of the track models on the high frequency components was considerably lessened. The inclusion of Ballast Track Model III (Fig. 10), for instance, did not significantly modify the computed response acceleration.

Viaduct 12 presented a much more complex behaviour when compared to the other two viaducts, since it was skewed and both twin slabs had to be modelled. Moreover, torsion was always present in all mode shapes. In the analysis presented here, the response of the deck was due to the moving forces acting on the opposite deck.

The response acceleration histories for a single locomotive (type 1116) are compared in Fig. 11. As the locomotive passed over one of the twin decks with a speed of 150 km/h, the numeric and measured responses were obtained on the opposite deck. For the other two viaducts, the influence of the vehicle mass and the nonlinear effects on the first natural frequency were observed as well. It was also observed that, when Track Model III was included, maximum accelerations were reduced and compared better with the measured response. The Fourier spectrum of the acceleration computed with Track Model III (Fig. 12) showed some dissipation of the higher frequencies but was not decisively different when compared to the response computed without the track model.

7. Conclusions

The main purpose of this paper is to present some results concerning the investigation of the dynamic response of medium-span railway viaducts, namely the influence of superstructure defined by the ballast track and the methodology applied for the load modelling. Two loading models were used: the Moving Forces and the Train–Structure Interaction models. Three different models for the track were investigated. The comparison was made using three real structures, for which the modal parameters and the acceleration response under real traffic were available. The computed response acceleration was systematically compared in the time domain with the measured response for the same type of vehicle passing over each of the viaducts. The influence of the track models was analysed mainly in the frequency domain and compared with the response obtained when no track model was included.

The dynamic behaviour of the finite element models of the viaducts showed very good agreement with the measurements. The time domain calibration using the response-accelerations measurements of the viaducts confirmed that time variation of the first natural frequency was necessary to reproduce the measured time histories, including forced and subsequent free vibration. Variations of the mass during the passage of trains and nonlinear behaviour of the ballasted track were thought to be responsible for this time dependency.

The numerical responses of the bridges, considering the track/bridge or vehicle/track/bridge systems, showed that the influence of track models was perceptible in the time domain only for the maximum accelerations. When response was analysed in the frequency domain, results showed that, for frequencies up to about 10–15 Hz, the different dynamic track models did not influence the frequency content, but for higher frequencies, the models acted as a filter. This effect was more consistent when using Track Model III and the Interaction load model. When using the Moving Forces load model, the effect of the track models was consistent with the previous conclusion but less significant.

These conclusions were clearly visible for one of the case studies (Viaduct 1), but the differences between separate track models and the differences between each model and the use of no model were much smaller.

Taking into account the relative contribution of frequency components greater than 15 to 20 Hz (which tend to be considerably less than those in the lower frequency range), the practical use of these type of track models did not seem to be meaningful since, according to EN 1990 [6], it is necessary to verify the peak deck acceleration. Moreover, the limit imposed by the code (which requires that the frequency band considered in the dynamic calculations should range from 0 to 30 Hz) should be reduced to 20 Hz to allow for the stability of the results for all of the models used in the computations.

The computations and the measurement results presented in this paper do not reflect the situation of resonance when the trains pass over the bridges with velocities near the critical value. Although this deserves further investigation in order to clarify the contribution of the ballasted track to the dynamic response of the bridges in that extreme situation, some preliminary results obtained during the analysis showed that the conclusions should not be considerably different.

References

[1] ADINA R & D, Inc, ADINA, Automatic dynamic incremental non linear analysis, USA. 2005.
[2] F. Armero, E. Petőcz, Formulation and analysis of conserving algorithms for frictionless dynamic contact/impact problems, *Computers Methods in Applied Mechanics and Engineering* 158 (1998) 269–300.
[3] K.J. Bathe, *Finite Element Procedures*, Prentice-Hall, 1996.
[4] K.J. Bathe, A Chaudhary, A solution method for planar and axisymmetric contact problems, *International Journal for Numerical Methods in Engineering* 21 (1985) 65–88.
[5] CEN—European Committee for Standardization (2003). EN1991-2, Actions on structures—Part 2: General actions—Traffic loads on Bridges.
[6] CEN—European Committee for Standardization (2005). EN1990—Annex A2, Basis of structural design – Annex A2 – Application for bridges (Normative).
[7] Y.S. Cheng, F.T.K. Au, Y.K. Cheung, Vibration of railway bridges under a moving train by using vehicle/track/bridge element, *Engineering Structures* 23 (2001) 1597–1606.
[8] ERRI D214/RP9., 1999. Rail bridges for speeds > 200km/h—Final report, European Rail Research Institute, ERRI.
[9] C. Esveld, *Modern Railway Track*, MRT-Productions, Germany, 1989.
[10] L. Fryba, *Vibration of Solids and Structures Under Moving Load*, 3rd edition, Thomas Telford, London, 1999.
[11] N. Hu, A solution method for dynamic contact problems, *Computers & Structures* 63 (6) (1997) 1053–1063.
[12] K. Knothe, S.L. Grassie, Modelling of railway track and vehicle/track interaction at high frequencies, *Vehicle System Dynamic* 22 (1993) 209–262.
[13] G.R. Love, T.A. Laursen, Improved implicit integration for transient impact problems—dynamic frictional dissipation within an admissible conserving framework, *Computers Methods in Applied Mechanics and Engineering* 192 (2003) 2223–2248.
[14] A. Man, A survey of dynamic railway properties and their quality, PhD thesis, TU Delft, DUP—Science, Delft. 2004.

[15] K. Popp, et al., Vehicle track dynamics in the mid-frequency range, *Vehicle System Dynamic* 31 (1999) 423–464.
[16] C. Rebelo, M. Hieden, M. Pircher, L. Simões da Silva, Vibrations measurements on existing single span concrete viaducts in Austria. EURODYN 2005, Paris, pp. 1637–1642.
[17] C. Rebelo, L. Simões da Silva, C. Rigueiro, M. Pircher, Dynamic behaviour of twin single-span ballasted railway viaducts—Field measurements and modal identification, *Engineering Structures* 30 (9) (2008) 2460–246910.1016/j.engstruct.2008.01.023.
[18] C. Rigueiro, C. Rebelo, L. Simões da Silva, Vibration of the railway track–viaduct system under moving vehicles taking to account the interaction effect, ISMA2006, pp. 1233–1248, Leuven.
[19] Xia H, Dynamic analysis of railway bridge under high speed trains, *Computers & Structures* 83 (1–4) (2005) 1891–1901.
[20] Y.B. Yang, J.D. Yau, Y.S. Wu, *Bridge interaction dynamics with applications to high-speed railway*, World Scientific, 2004.
[21] M. Zhai, Y. Wang, H. Lin, Modelling and experiment of railway ballast vibrations, *Journal of Sound and Vibration* 270 (2004) (2003) 673–683.
[22] N. Zhang, Vehicle–bridge vibration analysis under high-speed trains, *Journal of Sound & Vibration* 268 (2008) 103–113.